MILKY WAY GALAXY

Mapping spiral structure on the far side of the Milky Way

Alberto Sanna,[1]* Mark J. Reid,[2] Thomas M. Dame,[2] Karl M. Menten,[1] Andreas Brunthaler[1]

Little is known about the portion of the Milky Way lying beyond the Galactic center at distances of more than 9 kiloparsec from the Sun. These regions are opaque at optical wavelengths because of absorption by interstellar dust, and distances are very large and hard to measure. We report a direct trigonometric parallax distance of $20.4^{+2.8}_{-2.2}$ kiloparsec obtained with the Very Long Baseline Array to a water maser source in a region of active star formation. These measurements allow us to shed light on Galactic spiral structure by locating the Scutum-Centaurus spiral arm as it passes through the far side of the Milky Way and to validate a kinematic method for determining distances in this region on the basis of transverse motions.

Large-scale maps of the Milky Way have had to exclude a triangular region with the Sun at its apex and extending ~10° to either side of the Galactic center [e.g., (*1*)]. In this region, the Galaxy is rotating almost perpendicularly to our line of sight, so the radial velocities that enable the estimate of so-called kinematic distances are degenerate at values around zero. Some progress has been made in the nearer parts of this region with distances determined through stellar spectra and, more recently, parallax measurements for astronomical sources of maser emission from newly formed stars (*2*). But, the region behind the Galactic center has remained largely out of reach owing to the large distances (>9 kpc), very high foreground extinction, and source confusion.

The Bar and Spiral Structure Legacy (BeSSeL) Survey is a key project of the Very Long Baseline Array (VLBA), which has been measuring trigonometric parallaxes and motions on the sky plane (hereafter, proper motions) of methanol and water masers associated with hundreds of high-mass star–forming regions in the Galaxy. Recently, the project focused mainly on distant regions to locate distant segments of the Galactic spiral arms. Here, we discuss the most distant of these sources, G007.47+00.05 (or IRAS 17591−2228), for which an accurate parallax distance was not previously available. The source lies on the far side of the Galaxy and appears to link the prominent Scutum-Centaurus spiral arm in the fourth Galactic quadrant with a distant molecular arm recently discovered in the first quadrant, dubbed the Outer Scutum-Centaurus (OSC) arm (*3*).

We used the VLBA to observe strong H_2O maser emission at 22.2 GHz from the star-forming region G007.47+00.05 between March 2014 and March 2015 (*4*). We modeled the relative position in time of compact maser spots, with respect to an extragalactic continuum source (Fig. 1A), as the sum of the parallax signature (i.e., a sinusoid), caused by our changing vantage point as Earth orbits the Sun, plus a linear motion of the star-forming region relative to the Sun in the east-west and north-south directions (Fig. 1B). After removing the linear motion, the parallax effect inferred from this analysis (Fig. 1C) yields a parallax angle of 0.049 ± 0.006 milli-arcsec (mas). This measurement corresponds to a distance of

[1]Max-Planck-Institut für Radioastronomie, Auf dem Hügel 69, 53121 Bonn, Germany. [2]Harvard-Smithsonian Center for Astrophysics, 60 Garden Street, Cambridge, MA 02138, USA.
*Corresponding author. Email: asanna@mpifr-bonn.mpg.de

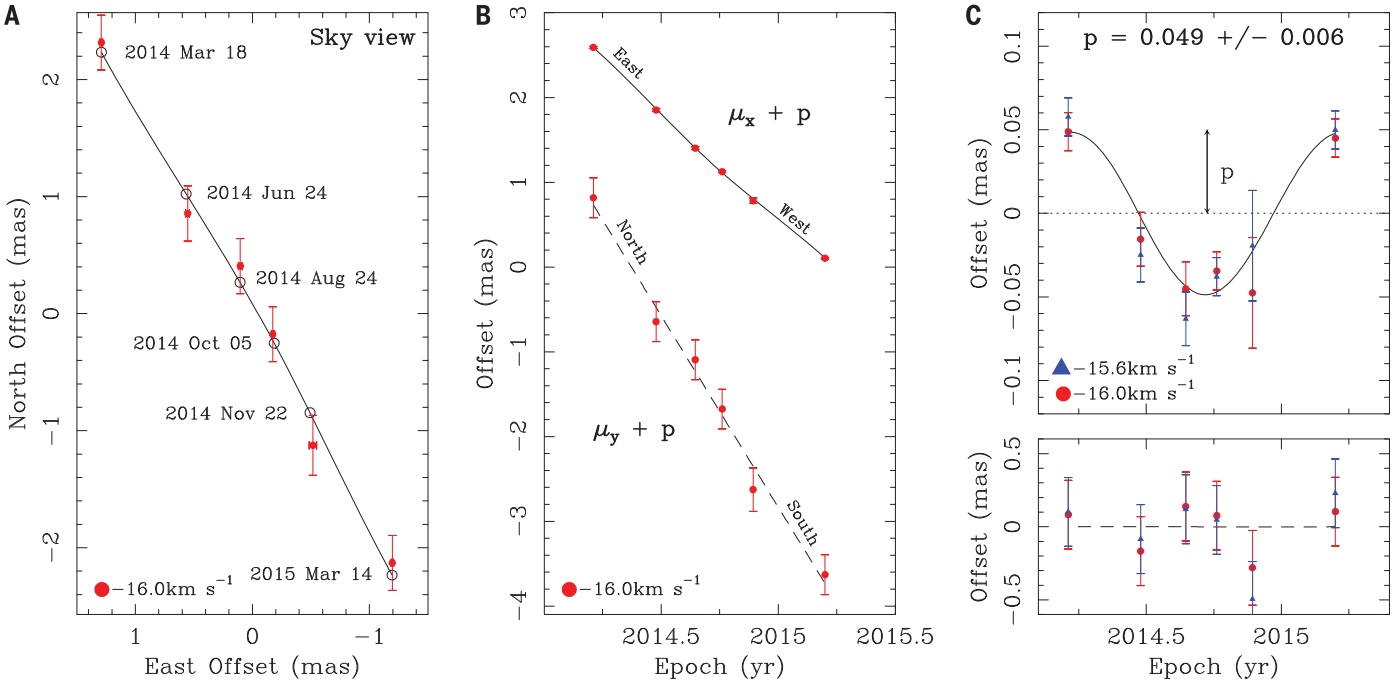

Fig. 1. Results of the combined parallax fit for G007.47+00.05. This fit is obtained from the combination of two point-like maser spots with respect to the background quasar J175526.28−223210.6 (or [IBR2011] J1755−2232; table S2). For clarity, we draw only maser positions for the spot at V_{LSR} of −16.0 km s^{-1} (red circles). (**A**) Sky-projected motion of the maser source with respect to J175526.28−223210.6 with each epoch labeled (the zero position is arbitrary). The empty circles and the line show the best-fitting position offsets and the trajectory, respectively. East offset uncertainties are smaller than the symbol. (**B**) Decomposed offset positions for the maser source along the east and north directions versus time. The best-fitting models in east and north directions are shown as continuous and dashed lines, respectively. (**C**) Same as the middle panel but with fitted proper motions subtracted (μ_x and μ_y), yielding the parallax sinusoid. Positions for the spot at V_{LSR} of −15.6 km s^{-1} are also shown for the final parallax (p). The east offset (upper panel) and north offset (lower panel) data are shown separately on different scales.

Table 1. Parameters used to calculate the distance PDFs. Column 1 gives the type of Galactic rotation curve adopted for the calculation [table 5 of (*2*)]. Columns 2 and 3 report the fundamental Galactic parameters of circular rotation speed at the solar circle and the distance of the Sun from the Galactic center, respectively (*2*). Columns 4 and 5 give the Galactic coordinates of the source in the longitude and latitude directions, respectively. Columns 6, 7, and 8 give the local standard of rest velocity of the source, and its motions on the sky plane, respectively.

Priors			Input data				
$\Theta(R)$	Θ_0 (km s^{-1})	R_0 (kpc)	ℓ (°)	b (°)	V_{LSR} (km s^{-1})	μ_x (mas year^{-1})	μ_y (mas year^{-1})
Universal	241 ± 8	8.34 ± 0.16	7.471	0.058	−16 ± 4	−2.44 ± 0.07	−4.51 ± 0.17

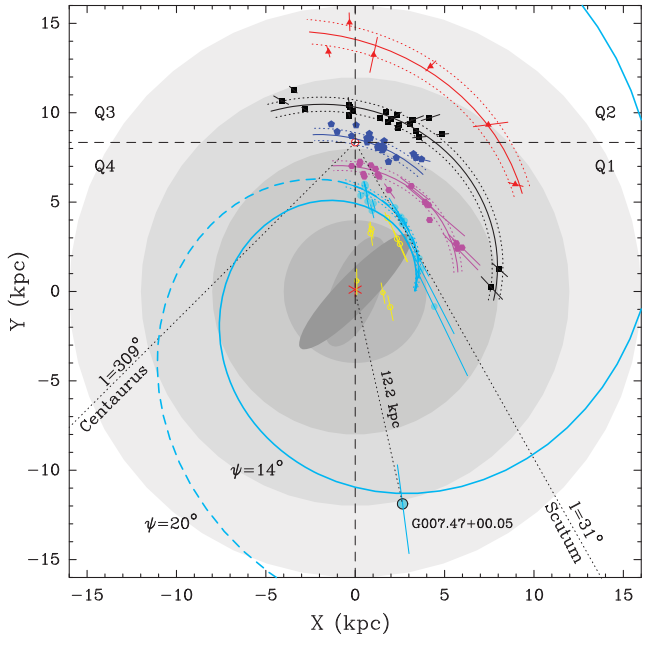

Fig. 2. Plan view of the Milky Way showing the location of G007.47+00.05 and other maser sources determined via trigonometric parallaxes [table 1 of (*2*)]. The reference system gives offset positions from the Galactic center (red asterisk). Colored symbols designate distinct regions in the Galaxy: inner Galaxy sources (empty yellow circles); Scutum-Centaurus arm (solid cyan circles); Sagittarius arm (magenta hexagons); Local arm (blue pentagons); Perseus arm (black squares); and Outer arm (red triangles). Error bars correspond to distance uncertainties of 1σ. The background gray disks, centered on the Galactic center, show regions within Galactocentric radii of 4, 8, 12, and 16 kpc. The Sun is located at (0, 8.34) kpc. Galactic quadrants, centered on the Sun, are indicated with dashed lines. Solid lines trace log-periodic spiral fits to sources grouped by arms; dotted lines correspond to 1σ widths. Two logarithmic spirals are drawn for the Scutum-Centaurus arm, one with a pitch angle (ψ) of 14° (solid), constrained by the Scutum and Centaurus tangent directions (*3*), and the other with a pitch of 20° (dashed), based on maser sources in the inner first quadrant (*14*). The Scutum and Centaurus tangent directions are also shown. [Adapted from figure 1 of (*2*)]

$20.4^{+2.8}_{-2.2}$ kpc (66,500 light years) with an uncertainty of less than ±14%. In Fig. 2, we plot the Galactic position of G007.47+00.05, superposed on a plan view of the Milky Way, which shows the locations of prominent star-forming sites determined from trigonometric parallaxes.

We compare this result with an independent, statistical (Bayesian), distance estimate (*5*), derived by taking into account complementary information about the spatial distribution and kinematics of giant molecular clouds in the Galaxy. In Fig. 3, we plot the probability density function (PDF) for the source distance, based on five distinct contributions (listed below), and the cumulative best estimate for the probability of any given distance (black solid line). The red solid line (PDF_{SA}) quantifies the probability that a set of three values—Galactic longitude (ℓ), latitude (b), and radial velocity with respect to the local standard of rest (LSR), V_{LSR}—match those values expected for a given spiral arm segment, as traced by CO and H I emission [e.g., (*6*)]. The loci of individual spiral arms are then fixed in position by trigonometric parallaxes, following previous analysis (*2*). Also plotted is the kinematic distance probability (PDF_{KD}), as inferred from the radial velocity of the source with respect to the Sun (V_{LSR}), after assuming a rotation curve for the Galaxy (*2*). Because star-forming regions are expected to lie close to the Galactic plane, we have also quantified the expectation of finding a source at high Galactic latitude if it is near the Sun, and vice versa (PDF_{GL}). Details of how these contributions are calculated have been previously discussed (*5*).

In Fig. 3, we assign two additional distance PDFs to the source, based on its proper motion in the Galactic latitude and longitude directions. The more distant the source, the smaller one expects the angular motion out of the plane ($PDF_{PM,b}$). At the same time, the proper motion along the plane (i.e., in Galactic longitude) provides an additional kinematic distance probability ($PDF_{PM,\ell}$), which makes use of the velocity component ($V_\perp$) perpendicular to the line of sight [e.g., (*7*)]. The probability density function, $PDF_{PM,\ell}$, is generated similarly to the PDF_{KD} [(*5*), section 2.2]. The observed proper motion components (μ_x, μ_y) are rotated about the line of sight into Galactic components (μ_ℓ, μ_b), and the component projected along the Galactic longitude (μ_ℓ) is compared with that expected under the assumption of circular Galactic orbits as a function of distance [e.g., equation 4 of (*7*)]. This calculation of kinematic distance using proper motions is most effective toward the Galactic center and anticenter, the directions in which conventional kinematic distances based on radial velocities are least useful. A similar calculation was previously followed by (*8*), who estimated for G007.47+00.05 a far kinematic distance of 20 ± 2 kpc (see supplementary text). These authors made use of the Japanese VERA (VLBI Exploration of Radio Astrometry) array to observe the H_2O maser emission between March 2009 and December 2011.

Evaluating the kinematic distance PDFs requires Bayesian priors for the Galactic rotation curve, $\Theta(R)$, and the fundamental Galactic parameters of the circular rotation speed Θ_0 at the distance R_0 of the Sun from the Galactic center. In Table 1, we list the priors and source input data used to calculate the PDFs. For the V_{LSR} of the source, we adopt the average velocity of the H_2O maser emission of −16 ± 4 km s^{-1}, which is consistent with the peak of radio recombination lines at −16.9 ± 0.1 km s^{-1} (*9*) and the range of CS emission at −13.9 ± 4.6 km s^{-1} (*10*). For the proper motion of the star-forming region (μ_x, μ_y), we averaged the final values derived from Fig. 1 (−2.42 ± 0.02 mas year^{-1}, −4.64 ± 0.30 mas year^{-1}) with those measured by (*8*) based on three masers (−2.46 ± 0.14 mas year^{-1}, −4.38 ± 0.14 mas year^{-1}). Because residual atmospheric delays between the target and calibration source usually dominate the uncertainty in proper motion measurements, and the three masers likely have the same systematic uncertainties, we have inflated by $\sqrt{3}$ the proper motion uncertainties from (*8*), to account for fully correlated motions among the masers. This analysis provides a proper motion in Galactic longitude (μ_ℓ) of −5.12 ± 0.18 mas year^{-1}.

In Fig. 3, we show that the combined Bayesian distance of 20.4 ± 0.6 kpc agrees well with our trigonometric parallax measurement. However, some caveats should be noted. Kinematic distances hold under the assumption of purely circular orbits. This condition is not satisfied within about 4 kpc of the Galactic center, where the

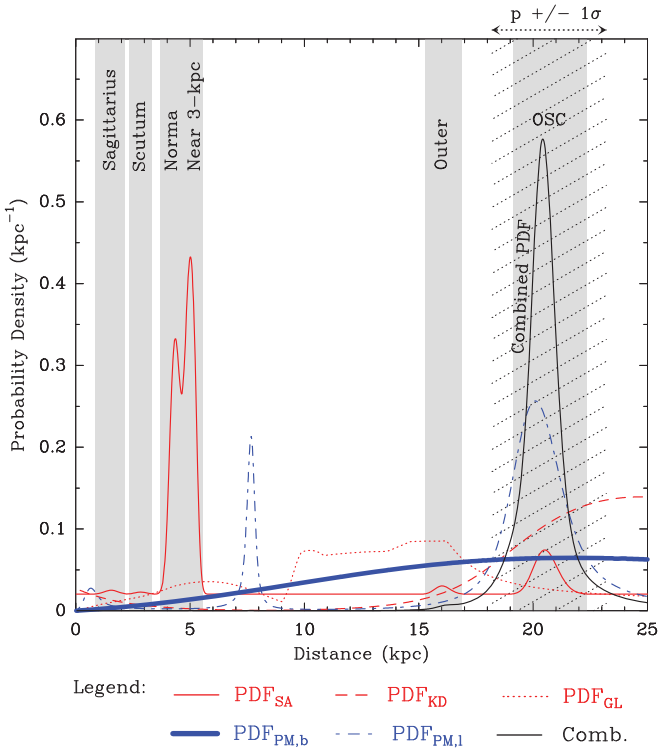

Fig. 3. Distance probability density function (PDF) for the star-forming region G007.47+00.05. Individual PDFs are indicated by subscripts and refer to the spiral arm assignment of the source (SA), its kinematic distance (KD), Galactic latitude (GL), and its proper motion in latitude (PM, *b*) and longitude (PM, ℓ). Input parameters for the PDFs are given in Table 1. Gray areas mark the expected regions for each spiral arm at a Galactic longitude of 7.5°. The combined PDF (black solid line) strongly favors an association with the Outer Scutum-Centaurus (OSC) arm at a distance of 20.4 ± 0.6 kpc. This estimate agrees with the trigonometric parallax distance of $20.4^{+2.8}_{-2.2}$ kpc (hatched black area).

gravitational effects of the Milky Way's central bar cause highly noncircular motions [e.g., (*11*, *12*)]. A line of sight from the Sun at $\ell = 7.47°$ passes through this region between 4.7 and 12.3 kpc; hence, this range of distances cannot be excluded on the basis of kinematic PDFs. Our direct parallax measurement does not suffer this limitation.

The spiral arm PDF (PDF$_{SA}$) has two main peaks between 4 and 5 kpc, because the target source has a V_{LSR} between that of the Norma (~10 km s^{-1}) and Near 3-kpc (−20 km s^{-1}) arms at that longitude [e.g., figure 7 of (*12*)]; the current parallax measurement unambiguously rules out such small distances. Distances to spiral arms beyond about 10 kpc are a substantial extrapolation because of the current lack of direct parallax measurements. The spiral arm PDF shows a small peak at ~16 kpc based on a long extrapolation of the Outer arm (red curve in Fig. 2) through the first Galactic quadrant. However, locating G007.47+00.05 at this distance can be excluded by the parallax distance, with a probability of >95%, as well as by kinematic distance values, because this portion of the Outer arm is well outside the Galactic center region.

Close to the Galactic plane at a longitude of 7.5° [e.g., figure 3 of (*3*)], the OSC arm has a V_{LSR} (–12 km s^{-1}) close to that of the target source. If the Scutum-Centaurus arm is a logarithmic spiral with constant pitch angle (ψ) of 14°, which is constrained by the tangent directions of the Scutum $\ell = 31°$ and Centaurus $\ell = 309°$ arms in addition to nearby parallax measurements (*3*), the distance to the OSC arm at the longitude of the maser source would be in the range of 20 to 21 kpc. In Fig. 2, we show the logarithmic spiral of the OSC arm under these conditions. This arm also coincides, within the uncertainties, with the farthest arm traced by (*13*), taking into account the value of R_0 adopted by those authors. This distance estimate determines a third peak of the PDF$_{SA}$ which is consistent with the trigonometric parallax distance. In Fig. 3, the combination of spiral and (both) kinematic PDFs strongly constrains a narrow range of distances (absolute peak of the black solid line), which matches the trigonometric distance of 20.4 kpc.

This result has two further consequences. First, the agreement of the parallax and the kinematic distances can be interpreted as evidence that the approximation of circular motions holds at Galactocentric radii near 12 kpc in the far outer Galaxy. Second, it calls into question the assumption of constant pitch angle of the Outer Scutum-Centaurus arm along its winding around the Galaxy. In Fig. 2, we extend the track of the Scutum segment from the first Galactic quadrant through the fourth quadrant, by assuming a logarithmic spiral with ψ of 20°. This pitch angle provides the best spiral fit to trigonometric distances of star-forming regions in the Scutum arm between ℓ of 5.9° and 32.0° (*14*, *15*). Because the near segment of the Scutum-Centaurus arm (i.e., the Scutum arm in the first quadrant) has a much larger pitch angle than that determined from the Scutum and Centaurus tangents and the location of G007.47+00.05 (14°), it is clear that a single logarithmic spiral cannot describe the full complexity of the Scutum-Centaurus-OSC arm. This result agrees with a recent analysis of the spiral arm morphology in four external face-on galaxies, where pitch angles can vary along individual arms by more than 10° (*16*).

In summary, we have measured the distance to a water maser source in the OSC arm using both a direct trigonometric parallax and a statistical Bayesian analysis. Our parallax distance agrees with an indirect distance estimate for the source inferred from its measured (proper) motion on the sky (*8*), thus providing support for the determination of kinematic distances based on proper motions rather than radial motions alone. These measurements allow us to trace the Scutum-Centaurus arm nearly one full turn of Galactic azimuth and out to large Galactocentric radii on the far side of the Milky Way, and show that we can map spiral structure throughout the Galaxy.

REFERENCES AND NOTES

1. J. H. Oort, F. J. Kerr, G. Westerhout, *Mon. Not. R. Astron. Soc.* **118**, 379–389 (1958).
2. M. J. Reid *et al.*, *Astrophys. J.* **783**, 130 (2014).
3. T. M. Dame, P. Thaddeus, *Astrophys. J.* **734**, L24 (2011).
4. Materials and methods are available as supplementary materials.
5. M. J. Reid, T. M. Dame, K. M. Menten, A. Brunthaler, *Astrophys. J.* **823**, 77 (2016).
6. T. M. Dame, D. Hartmann, P. Thaddeus, *Astrophys. J.* **547**, 792–813 (2001).
7. Y. Sofue, *Publ. Astron. Soc. Jpn.* **63**, 813–821 (2011).
8. A. Yamauchi *et al.*, *Publ. Astron. Soc. Jpn.* **68**, 60 (2016).
9. D. S. Balser, R. T. Rood, T. M. Bania, L. D. Anderson, *Astrophys. J.* **738**, 27 (2011).
10. L. Bronfman, L.-A. Nyman, J. May, *Astron. Astrophys. Suppl. Ser.* **115**, 81 (1996).
11. J. Binney, O. E. Gerhard, A. A. Stark, J. Bally, K. I. Uchida, *Mon. Not. R. Astron. Soc.* **252**, 210–218 (1991).
12. A. Sanna *et al.*, *Astrophys. J.* **781**, 108 (2014).
13. H. Nakanishi, Y. Sofue, *Publ. Astron. Soc. Jpn.* **68**, 5 (2016).
14. M. Sato *et al.*, *Astrophys. J.* **793**, 72 (2014).
15. V. Krishnan *et al.*, *Astrophys. J.* **805**, 129 (2015).
16. Z. N. Honig, M. J. Reid, *Astrophys. J.* **800**, 53 (2015).

ACKNOWLEDGMENTS

A.S. gratefully acknowledges financial support by the Deutsche Forschungsgemeinschaft (DFG) Priority Program 1573. The National Radio Astronomy Observatory is a facility of the National Science Foundation operated under cooperative agreement by Associated Universities, Inc. This work made use of the Swinburne University of Technology software correlator, developed as part of the Australian Major National Research Facilities Programme and operated under license. We thank M. Honma for fruitful discussions in preparation. All data used in the paper are available through the National Radio Astronomy Observatory (NRAO) archive at https://archive.nrao.edu/archive/advquery.jsp under program BR198. The spectrum of the maser emission on March 18 2014 is available at http://bessel.vlbi-astrometry.org/first_epoch.

SUPPLEMENTARY MATERIALS

www.sciencemag.org/content/358/6360/227/suppl/DC1
Materials and Methods
Supplementary Text
Figs. S1 and S2
Tables S1 to S3
References (*17*–*31*)

28 April 2017; accepted 5 September 2017
10.1126/science.aan5452

Mapping spiral structure on the far side of the Milky Way

Alberto Sanna, Mark J. Reid, Thomas M. Dame, Karl M. Menten and Andreas Brunthaler

Science **358** (6360), 227-230.
DOI: 10.1126/science.aan5452

Measuring the far side of the Galaxy

Direct measurements of distances to astronomical sources rely on parallax, which can usually only be measured for relatively nearby objects. The far side of the Milky Way has been impossible to measure accurately, because the parallax is very small and interstellar dust blocks optical light from those regions. Sanna *et al.* used radio interferometry to directly determine the parallax distance to a star-forming region on the far side of the Galaxy. They also used a method of inferring distances from transverse motions, which produced the same answer. This allowed them to trace one of the Milky Way's spiral arms through almost an entire rotation.

Science, this issue p. 227